

INFLUENCE OF OPTICAL AND GEOMETRICAL PARAMETERS ON SCINTILLATION
DETECTION IN GAMMA CAMERA HEADS

M. Jatteau and G. Normand
Laboratoires d'Electronique et de Physique appliquee,
3, avenue Descartes, 94450 Limeil-Brevannes, France

ABSTRACT

By using a computer simulation program developed for the study of the light collection by photomultiplier tubes in scintillation cameras, the influence of various optical and geometrical parameters of the camera head on the scintillation detection process is examined. In particular, the effect of useful parameters for camera head design such as light guide thickness, photocathode diameter and scintillating crystal, on the PMT response as a function of the distance "scintillation point - PMT axis" are given. Some parameters inaccessible to experimentation are computed such as the relative contribution of direct light to the total amount collected by PM tubes, the distribution of incidence angles of photon tracks reaching the photocathodes as well as the photon irradiance over the output plane of the camera optical block. In addition, the computed statistical results delivered by this simulation program allow appraisal of the practical limits of the intrinsic spatial resolution of scintillation cameras.

INTRODUCTION

Due to the large development of data and image processing systems interfaced to gamma-ray cameras¹, and the introduction of Single Photon Emission Computerized Tomography techniques², one of the trends in Nuclear Medicine is towards quantitative examinations³. That means gamma-ray detectors designed to be imaging systems are also measuring instruments able to process spectrometry and counting information simultaneously. During the last ten years, many efforts have been made by the camera manufacturers to improve the intrinsic qualities of scintillation cameras. Some of the detector defects such as linearity distortions, field of view nonuniformities, and instabilities of

response can be significantly reduced by means of micro-computer based correction systems^{1,4}. Some other characteristics such as maximum true count-rate, spatial resolution and spectral selectivity may be understood through studies respectively of the data acquisition electronics or of the physical part of camera heads.

Within the context of such an optimization study made at LEP⁵, a computer simulation program for the light collection process in scintillation cameras has been developed and tested⁶. In addition to output data which can be compared to experimental values (a good agreement is shown⁶), this program can deliver other computed results which cannot be easily obtained experimentally on a camera head although they can be very useful. The use of this approach to study the influence of various parameters on scintillation detection in gamma camera heads is presented in this paper. Some other computed results which appraise the physical limits of performance parameters such as practical intrinsic spatial resolution on scintillation cameras will be also considered below.

REVIEW OF THE COMPUTER SIMULATION PROGRAM

The computer simulation program for the light collection process in scintillation cameras, based on the Monte Carlo method, is described in detail in another paper⁶. The main phenomena taken into account in the physical model from the interaction of a gamma quantum within the scintillating crystal is either the emission of one primary electron by the PMT photocathodes or the photon absorption are summarized by the block diagram given in figure 1.

1. Input data

The geometrical and physical parameters of the optical block have to be fixed according to the camera head configuration under consideration. The input data file includes:

- a) the coordinates of the gamma-ray beam (X,Y) and the energy (E) of the gamma quanta.
- b) the thickness and refractive index of the scintillating crystal (t_1, n_1), light guide (t_2, n_2) and photoemissive layer ($t_3, n_3+i k_3$) for the mean wavelength corresponding to the

scintillation light.

- c) the number of PM tubes (N) and their location according to the arrangement over the field of view and the useful (ϕ_{pK}) photocathode diameter and external (ϕ_{ex}) PMT diameter.
- d) the reflection factor of the entrance scattering plane (ρ_e) and the area located outside the photocathodes (ρ_a) with an optional reflection law according to the optical treatment considered.
- e) the linear absorption coefficients of the crystal, μ_γ for the gamma ray beam of energy E, μ_c for the scintillation light and μ_g for the light guide.

2. Computed results

The computed results can be directly compared to experimental values⁶ such as the number of primary photoelectrons emitted by the photocathodes, whose mean value is closely related to the mean PMT output signals and the standard deviation which is related to the respective FWHM energy resolution. Other computed results cannot be easily obtained experimentally. In this paper, some of the following are considered.

- a) the amount of "direct" light detected or collected by the PM tubes, i.e. the numbers of photons absorbed by the photocathodes (n_{AD}) or those reaching them (n_{ID}) directly from the scintillation point without any reflection. From n_{AD} the number of photoelectrons emitted, N_D , can be deduced.
- b) the photon irradiance ($dn/d\sigma$) over the output plane of the optical block and its variation as a function of the distance (ρ) from the gamma ray beam axis; these results have been computed for $5 \times 5 \text{ mm}^2$ element area for total light and direct light. For each scintillation, the coordinates (x_b, y_b) of the barycentre of the two dimensional light distribution, $dn/d\sigma(\rho)$, can be deduced.
- c) the number of photons $n(\zeta)$ impinging on the output plane with incidence angles included into a given one degree range (from ζ to $\zeta + 1^\circ$) as a function of ζ . This result can be represented in the form of incidence angle distribution diagrams for total light as well as for direct light.

INFLUENCE OF VARIOUS PARAMETERS ON THE SHAPE OF "SIGNAL-DISTANCE"
CURVES

A "signal-distance" curve is defined as the normalized variation $S(d)/S(o)$ of the mean pulse height value corresponding to the output signal delivered by a photomultiplier tube as a function of the distance d from the scintillation point to the PMT axis. Such curves can be easily measured on a gamma camera head and comparisons under various conditions with the computed number of photoelectrons emitted by the photocathodes due to the total light (N_T) have been found to be in very good agreement⁶.

1. Direct light contribution

From computed mean values of $\overline{N}_D(d)$, the normalized variations $\overline{N}_D(d)/\overline{N}_D(o)$ provide information about the fraction of direct light contributing to the output PMT signal ($\overline{N}_T(d)/\overline{N}_T(o)$ "signal-distance" curve): figure 2. The computations have been made for a camera head provided with 37 photomultiplier tubes #2432 from RTC), with a NaI(Tl) crystal of thickness $t_1 = 12.5$ mm; for two light guide thicknesses (t_2) $t_2 = 16$ mm and $t_2 = 24$ mm. The value used for normalization is $N_T(o)$ for the case $t_2 = 24$ mm (curve 1).

2. Effect of light guide thickness

Figure 2 provides an estimate of the effect of the light guide thickness on the shape of "signal-distance" curves. Computed and experimental results have been found to be in very good agreement for a camera head configuration with a NaI(Tl) crystal thickness $t_1 = 6$ mm, a set of 37 x PM 2102 PMTs* and various light guide thicknesses⁶. Figure 3 shows the shape changes of the "signal-distance" curve (total light), computed for various values of t_2 , for a hypothetical camera head configuration provided with a NaI(Tl) crystal of $t_1 = 25$ mm and 37 x XP 2000 PMTs. Useful information for camera design drawn from these results is that the shape of such curves is mainly dependent on the depth "scintillation

* PM 2102, XP 2000 ($\varnothing_{ex} = 53$ mm) and PM 2432 ($\varnothing_{ex} = 60$ mm) are RTC products.

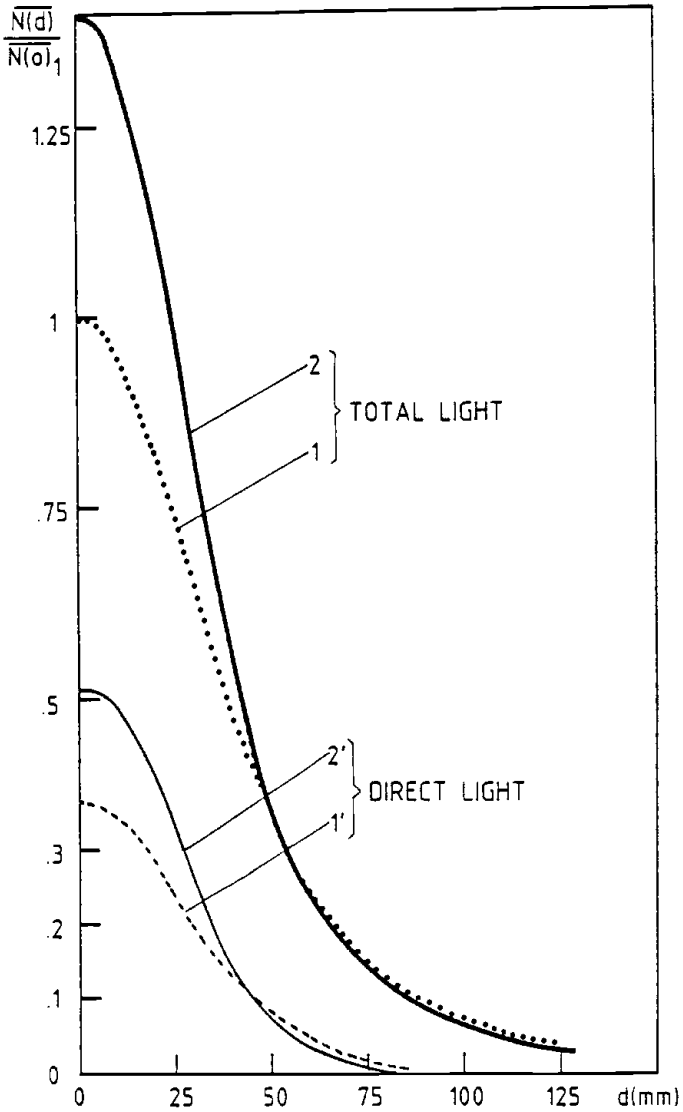


Figure 2. Normalized "signal-distance" curves for total light and direct light.

Camera head configurations (37 x PMT 2432):

1.1' : $T_1 = 12.5 \text{ mm}$; $t_2 = 24 \text{ mm}$

2.2' : $T_1 = 12.5 \text{ mm}$; $t_2 = 16 \text{ mm}$

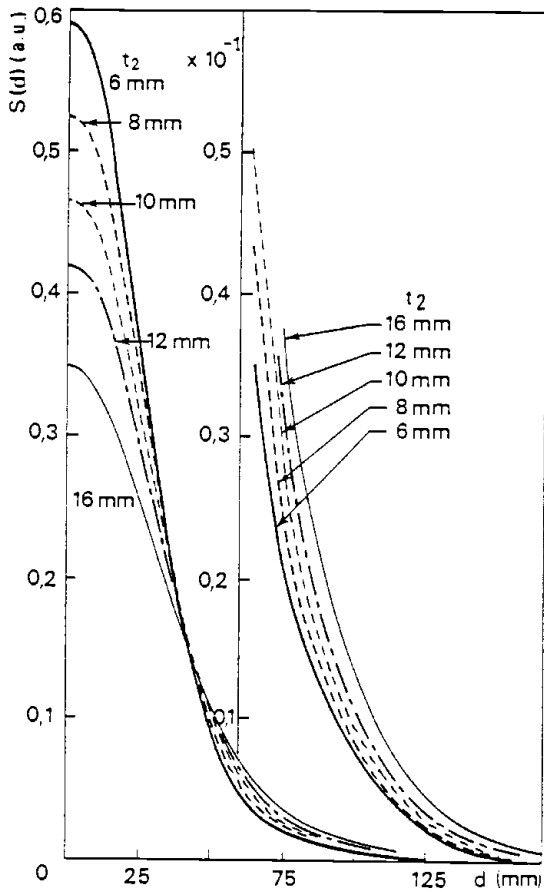


Figure 3. Computed effect of the light guide thickness (t_2) on the shape of "signal-distance" curves ($S(d)$ in arbitrary units); with $t_1 = 25$ mm, PMT : XP 2000 (from ref. 5).

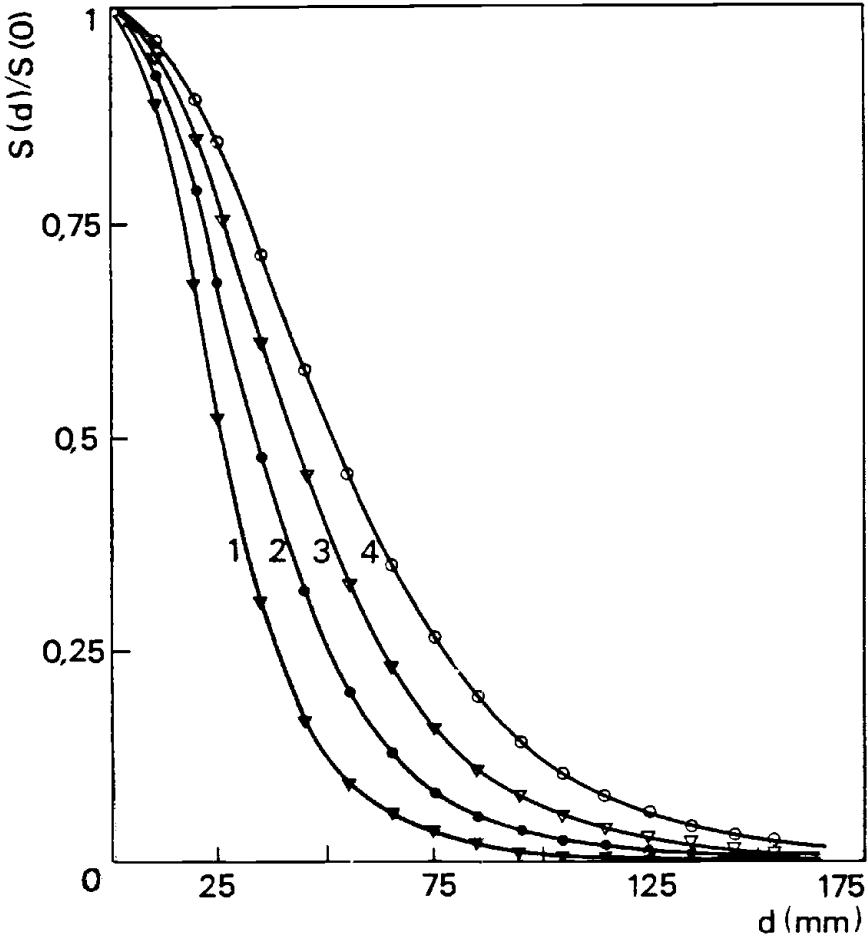


Figure 4. Computed influence of the PMT photocathode diameter (ϕ_{PK}) on the shape of normalized "signal-distance" curves (with $t_1 + t_2$ $\frac{t_1 + t_2}{\phi_{PK}} = \text{cte} = .69$; $\phi_{PK} 1 : 38 \text{ mm}$; 2: 51 mm; 3 : 63.5 mm; 4 : 76 mm)

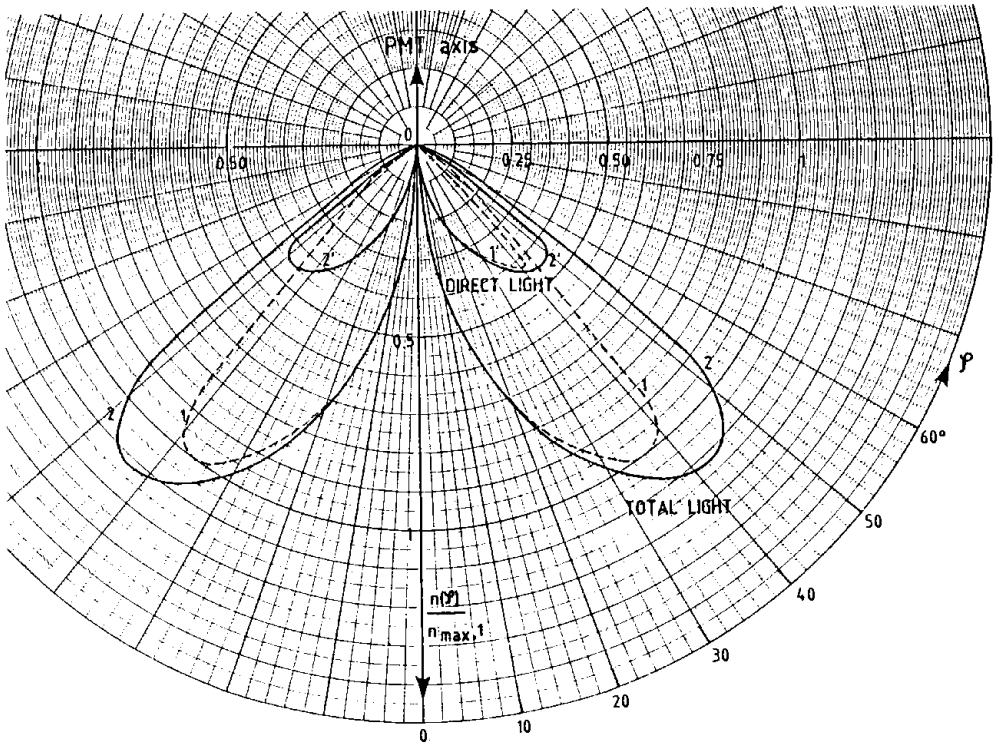


Figure 6. Computed incidence angle distribution diagrams related to the central PM tube ($d = 0$). Camera head configurations : see fig. 2.

point-photocathode plane".

3. Effect of PMT photocathode diameter

It is obvious that the shape of "signal-distance" curves depends on the PMT photocathode diameter ϕ_{PK} . Figure 4 shows this effect for 4 different values of ϕ_{PK} with a constant ratio between the total thickness of the optical block ($t_1 + t_2$) and the photocathode diameter ϕ_{PK} , assuming a given crystal ($t_1 = 12.5$ mm). The sharpness of the "signal-distance" curves increases when ϕ_{PK} decreases and is a favourable factor to improve the intrinsic spatial resolution of gamma-ray cameras.

4. Influence of the scintillating material

Figure 5 shows the influence on the light collection of the use of hypothetical large scintillator plates made of different material, such as calcium fluoride, cesium fluoride, and bismuth germanate of the same thickness. In fact, the changes in the shape of the normalized "signal-distance" curves are mainly due to the different values of refractive index without taking into account the respective light efficiencies. From these results, it is shown that a high refractive index is not favourable to the optimum collection of light by the photomultiplier tubes.

INCIDENCE ANGLE DISTRIBUTION AND PHOTON EMISSION DIAGRAMS

The computed variations of $n(\zeta)$ (as defined in "computed results"), and plotted as a function of ζ , correspond to the incidence angle distribution diagrams. Examples are given by figure 6 for the central PM tube of a camera head for a NaI(Tl) crystal ($t_1 = 12.5$ mm) and 37 x PM 2432*, for 2 light guide thicknesses ($t_2 = 16$ mm and 24 mm), when scintillations originated on the PMT axis ($d = 0$). The value used for normalization is $n(\zeta)_{\max}$ in the case of $t_2 = 24$ mm; note that these diagrams are figures of revolution around the PMT axis. They

* PM 2102, XP 2000 ($\phi_{ex} = 53$ mm) and PM 2432 ($\phi_{ex} = 60$ mm) are RTC products.

show that most of the photon tracks impinging on the photocathode of the central PM tube have incidence angles larger than 25 degrees. These diagrams show also the relative magnitudes of the direct light and total light.

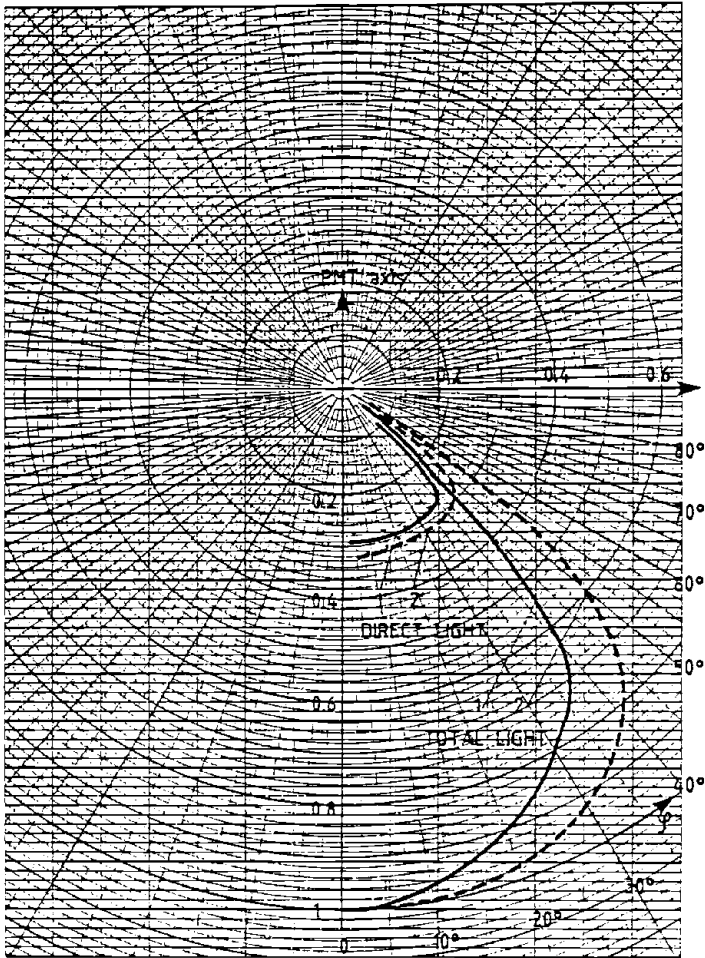


Figure 7. Computed photon emission diagrams related to the central PM tube ($d = 0$). Camera head configurations: see fig. 2.

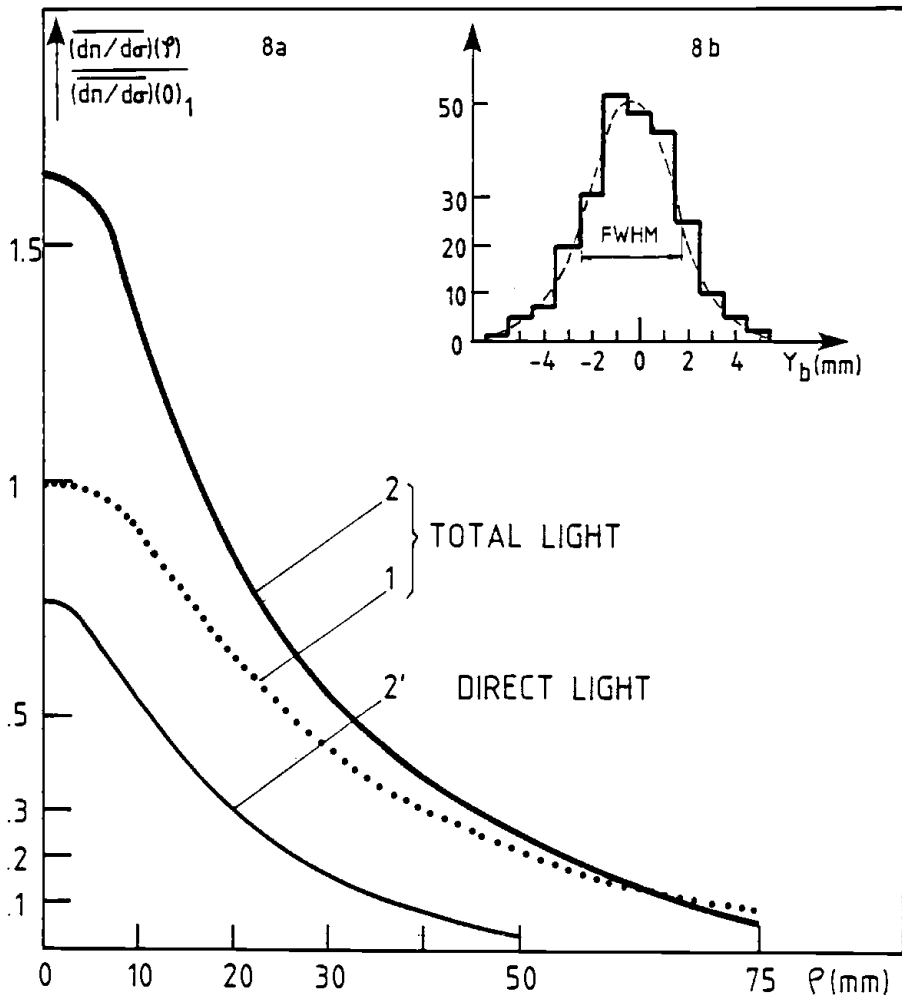


Figure 8a. Normalized variations of the photon irradiance $dn/d\sigma$ over the output plane of the optical block as a function of the distance (ρ) from the gamma-ray beam located at $d = 0$. (Camera head configurations: see fig. 2).

Figure 8b: Example of statistical distribution of computed y_b coordinates of the barycentre (250 scintillations located in $y = 0$).

From the results, taking into account the differential solid angle $d\omega = 2\pi \sin \zeta d\zeta$ related to each direction ζ (with $d\zeta = 1^\circ$), the photon emission diagrams at the output plane of the optical block can be deduced. Figure 7 gives an example of such emission diagrams related to the central PM tube, the scintillations originating on the PMT axis ($d = 0$), for direct and total light (note that they are also figures of revolution around the PMT axis). It is shown that inside the angular limits related to the photocathode size and light guide thickness, the direct light emission diagram is close to the isotropic law (used for photon emission from the scintillation point) and the total light emission diagram is similar to Lambert's law (used for photon emission at the input scattering plane).

LIGHT DISTRIBUTION CURVES AND APPLICATION

The distribution curves over the output plane of the optical block $dn/d\sigma(\rho)$ (as defined in the paragraph "computed results") have been computed for a large number of scintillations (S) located at the same place. The figure 8a gives the normalized variations of the mean value. $dn/d\sigma(\rho)$ as a function of ρ for direct and total light when the scintillations are located on the PMT axis ($d = 0$) (for the same conditions as the ones defined previously in "Direct light contribution"). The value used for normalization is equal to $dn/d\sigma(0)$ in the case $t_2 = 24$ mm. These results, related to photon irradiance variations over the output plane, are difficult to measure, but can be used from a theoretical point of view for evaluation of the limit of intrinsic spatial resolution (LISR) for a given camera head configuration.

According to the physical model used in our computer simulation program⁶, the statistical fluctuations of the computed light distribution curves for a series of (S) scintillations (j) introduce random coordinates x_{bj}, y_{bj} of their barycentre, around the respective mean values

$$\bar{x}_b = \frac{1}{S} \sum_{j=1}^S x_{bj} ; \quad \bar{y}_b = \frac{1}{S} \sum_{j=1}^S y_{bj}$$

Figure 8b gives an example of the statistical distribution of

these coordinates for a line source located at $Y = 0$, for a camera head configuration defined by $t_1 = 12.5$ mm, $t_2 = 24$ mm, 37×2432 PMTs. The averaged curve corresponding to this distribution represents the physical line spread function (LSF) which illustrates the inaccuracy of the response to a line source for this camera head without any other cause of errors due to the pulse arithmetics associated with this camera. Consequently the standard deviation

$$\sigma_{by} = \frac{1}{S} \sum_{j=1}^S (y_{bj} - \bar{y}_b)^2$$

of this distribution is related to the highest achievable resolving power of this camera, only limited by the physical random phenomena occurring in gamma-ray detection. The full-width-at-half-maximum (FWHM) of this distribution (see figure 8b) more commonly used in nuclear medicine instruments, is called the limit of intrinsic spatial resolution (LISR) for this camera. Assuming a gaussian distribution, $LISR_{\{FWHM\}} = 2.35 \sigma_b$. In the present case, we obtain $LISR = 4.2$ mm FWHM at 140 KeV.

As an example of the application of such an approach, the LISR values of low energy camera heads provided with a thin scintillating crystal ($t_1 = 6$ mm) and with a set of 53 mm external diameter photomultiplier tubes have been computed⁷ and are reported in the table below:

t_1 (crystal)	t_2 (light guide)	computed LISR (FWHM) at 140 KeV
6 mm	19 mm	$3 \pm .1$ mm
6 mm	10 mm	$2.5 \pm .1$ mm
6 mm	6 mm	$1.8 \pm .1$ mm

The first configuration ($t_1 = 6$ mm, $t_2 = 19$ mm) corresponds to an

optimized laboratory model of low-energy Anger camera, provided with 37 x 2 inch PMTs fabricated at LEP: the intrinsic spatial resolution has been found close to the computed LISR with intrinsic linearity distortions which have to be corrected by electronic means. The use of a thinner light guide ($t_2 = 10$ mm) in this camera model did not allow us to reach intrinsic spatial resolution better than 3 mm FWHM for 140 KeV photons. The last configuration which used a very close light coupling ($t_2 = 6$ mm) is only compatible with the design of image intensifier gamma-ray cameras, similar to the ones suggested by several investigators⁸⁻¹⁰. Experiments on such cameras revealed the necessity to do sophisticated corrections¹¹.

CONCLUSION

A method for investigation of the process of light collection by photomultiplier tubes in scintillation cameras by means of a computer simulation program has been developed at LEP. The study of the influence of various optical and geometrical parameters on the PMT response has been shown to be useful for optimal camera head design. The relatively small contribution of the light coming directly from scintillations to the signals delivered by the PM tubes has been shown. Diagrams of the incidence angle distribution related to the central PM tube of a gamma-camera head, as well as the corresponding emission diagrams have been computed for direct and total light. In addition, this program can be used to evaluate, under practical considerations, the limit of intrinsic spatial resolution for scintillation cameras.

ACKNOWLEDGEMENTS

We would like to thank the LEP Management who authorized the presentation of this paper especially Mr. J. Donjon for his encouragement and interest in this study.

REFERENCES

1. G. Muehllehner and J. Colsher, "Single Photon Imaging, New Instrumentation and techniques" in "Medical Radionuclide Imaging 1980", Vienna IAEA, Vol. 1, 173-198, 1981.
2. T.F. Budinger, "Physical Attributes of Single-Photon Tomography", J. Nucl. Med., 21, 579-592, 1980.
3. M. Jatteau, "Trends in Medical Radionuclide Imaging" in "Proceedings of EUROCON '80 Stuttgart", W. Kaiser and W.E. Proebster (eds), North-Holland Publishing Company, Amsterdam, 555-560, 1980.
4. G.F. Knoll, M.C. Bennet, K.F. Koral and D.R. Strange, "Removal of gamma camera nonlinearity and nonuniformities through real-time signal processing", in "Information Processing in Medical Imaging", R. Di Paola and E. Kahn (eds), Colloque INSERM, 187-200, 1979.
5. M. Jatteau, P. Lelong, G. Normand, J. Ott, J. Pauvert and J. Pergrale, "Pour une optimisation des cameras de gammagraphie de type Anger", Acta Electronica, 22, 2, 91-117, 1979.
6. G. Normand, M. Jatteau, P. Lelong and J. Ott, "Computer simulation of the light collection process in scintillation gamma-ray cameras" in "Advances in Scintillation Counting", S.A. McQuarrie, C. Ediss and L.I. Wiebe (Eds), University of Alberta Press, Edmonton, p. 176-189, 1983.
7. M. Jatteau, P. Lelong, G. Normand and J. Ott, "Limits of intrinsic spatial resolution in scintillation gamma-ray cameras", in "Nuclear Medicine and Biology", C. Raynaud (ed), Pergamon Press, Vol. II, 1526-1529, 1982.
8. A. Lansiaart, J. Lequais, G. Roux, J.P. Morucci and J.C. Gaucher, "Detecteur stationnaire a gaz et nouveau type de gammascopie", in "Medical Radioisotope Scanning", Vienna IAEA, Vol. 1, 87-98; 1969.
9. B. Conrad and W. Platz, "Le Scinticon, une nouvelle camera a scintillation", Electromedica, 4-5, 220-225, 1973.

10. G. Roziere, M. Verat, H. Rougeot and B. Driard, "Large field of view image intensifier gamma-camera detectors using a silicon XY scintillation localizer", IEEE Trans. on Nucl. Science, NS-28, 1, 60-63, 1981.
11. M.T. Blond, B. Aubert and R. Di Paola, "Computer corrections of image intensifier camera response", in "Information Processing in Medical Imaging", R. Di Paola and E. Kahn (eds), Colloque INSERM, 173-184, 1979.